J Neurol (2009) 256:916–924
DOI 10.1007/s00415-009-5040-7

ORIGINAL COMMUNICATION

In vivo mapping of incremental cortical atrophy from incipient to overt Alzheimer's disease

Giovanni B. Frisoni · Annapaola Prestia · Paul E. Rasser · Matteo Bonetti · Paul M. Thompson

Received: 13 September 2008 / Revised: 7 January 2009 / Accepted: 20 January 2009 / Published online: 28 February 2009

Abstract Progressive brain atrophy is believed to be the Alzheimer's disease (AD) marker with the greatest evidence for validity. Mapping the topography of cortical atrophy throughout the stages of severity may allow the neural networks affected to be identified. Twenty healthy elderly persons (OH, MMSE 29.1 ± 1.0), 11 patients with incipient AD (iAD, 26.5 ± 2.0), 15 with mild AD (miAD, 23.5 ± 2.2), and 15 with moderate AD (moAD, 16.5 ± 2.0) underwent 3D magnetic resonance. Cortical pattern matching analysis was performed and maps of percent differences in gray matter distribution were computed between the following groups: iAD versus OH, miAD versus iAD, and moAD versus miAD. Compared to OH, iAD patients exhibited a mean cortical gray matter loss of 9–20% in areas encompassing the polysynaptic hippocampal pathway (posterior cingulate/retrosplenial and medial temporal cortex) and subgenual/orbitofrontal cortices, and a less widespread loss of 5–11% in other neocortical areas. Compared to iAD, miAD featured widespread mean gray matter loss of 14–19% in areas encompassing the direct hippocampal pathway (temporal pole, temporoparietal association cortex, and dorsal prefrontal cortex), sensorimotor, and visual cortex, with a less marked loss (7–9%) in the polysynaptic pathway areas. Compared to miAD, only atrophy in the primary sensorimotor cortex was still relatively marked in moAD, with a mean gray matter loss of 10–11%; the loss in other regions was generally below 10%. These findings suggest that the polysynaptic hippocampal pathway is affected in iAD, the direct pathway and sensorimotor and visual networks are affected in moAD, and the sensorimotor network is affected in moAD.

Keywords Alzheimer's disease · Cortical pattern matching · Brain atrophy · Mild cognitive impairment (MCI) · Volumetric MRI

Electronic supplementary material The online version of this article (doi:10.1007/s00415-009-5040-7) contains supplementary material, which is available to authorized users.

G. B. Frisoni (✉) · A. Prestia
Laboratory of Epidemiology Neuroimaging and Telemedicine, IRCCS Centro San Giovanni di Dio FBF, The National Centre for Research and Care of Alzheimer's and Mental Diseases, via Pilastroni 4, 25125 Brescia, Italy
e-mail: gfrisoni@fatebenefratelli.it

G. B. Frisoni
Psychogeriatric Ward, IRCCS Centro San Giovanni di Dio FBF, The National Centre for Research and Care of Alzheimer's and Mental Diseases, Brescia, Italy

P. E. Rasser
Schizophrenia Research Institute, Sydney, Australia

P. E. Rasser
Priority Centre for Brain and Mental Health Research, School of Design, Communication and IT, University of Newcastle, Newcastle, Australia

M. Bonetti
Service of Neuroradiology, Istituto Clinico Città di Brescia, Brescia, Italy

P. M. Thompson
Laboratory of Neuro Imaging, UCLA School of Medicine, Los Angeles, USA

Introduction

Progressive atrophy is the disease marker in Alzheimer's with the greatest evidence for validity, and is the most promising surrogate outcome in clinical trials [1]. High-resolution magnetic resonance (MR) has been featured in

all phase III clinical trials with anti-amyloid agents. However, atrophy is regarded throughout the whole brain, while neuropathological evidence indicates a specific topography of plaque and tangle accumulation with increasing disease severity. Therefore, in vivo studies are necessary to map the topography of brain damage in untreated Alzheimer's disease (AD) patients at different disease stages that will provide a benchmark against which the efficacy of disease-modifying drugs can be judged.

Serial MR scans in persons with genetic forms of AD have estimated that the brain starts losing volume 3.5 years before AD diagnosis [2]. Whole-brain atrophy then progresses exponentially, accelerating at 0.26% per year, such that atrophy is progressing at 2.5–3% per year five years after diagnosis. This pattern is not uniform across the brain; atrophy in the hippocampus starts about two years earlier and five years after onset acceleration is almost twice that of the rest of the brain [2]. A recent region-of-interest (ROI) study confirmed this acceleration in patients with memory deficit later progressing to AD [3]. It is reasonable to assume that atrophy may not accelerate indefinitely, but that severity-related patterns of acceleration/deceleration might map to the neural networks involved in different stages of AD severity.

Different studies have addressed the issue of the topography of the progression of atrophy in AD. Serial imaging in patients with familial and sporadic AD has shown that tissue loss starts in the medial temporal lobe and later extends to frontal, temporal, and parietal neocortical regions [4], in agreement with the known progression of AD pathology [5]. Cross-sectional studies of sporadic late-onset AD have confirmed the same sequence [6]. Most of the available studies have used either ROI approaches, which have the limitation that only a few brain regions can be studied [7], or automated algorithm pipelines such as voxel-based morphometry [8], which is limited by a relatively low spatial resolution and a lack of anatomical detail for precise cortical localization.

The aim of this study is to map the topography of acceleration–deceleration of cortical atrophy from good health through to incipient, mild and moderate AD in order to gain insight into the neural networks that are affected throughout the stages of disease severity. A technique will be used (cortical pattern matching—CPM) that enables volumetric changes of the cortical mantle to be mapped with a spatial accuracy of a few millimeters.

Methods

Study subjects and assessment

Thirty AD were recruited from among those coming for observation at our Outpatient Memory Clinic in Brescia. Of the original group of 68 AD patients, we selected 15 with disease onset after age 65 whose illness severity was considered "mild" (MMSE score $\geq$ 20, miAD), and 15 whose disease severity was considered "moderate" (MMSE score $\leq$ 19, moAD). Incipient AD (iAD) patients were selected from a group of 60 with amnestic mild cognitive impairment (MCI) based on current research criteria [9] who had converted to AD and had a valid scan.

Patients were assessed between November 2002 and October 2007 and underwent history taking, laboratory exams, physical and neurological examination, neuropsychological assessment, and MR scanning. History was taken with a structured interview from patients' relatives (typically spouses); laboratory exams included genomic DNA extraction with APOE genotyping according to standard procedures. Neuropsychological assessment was performed by a psychologist and assessed (1) global cognitive functioning with the mini-mental state examination, (2) language with category fluency and token tests; (3) visuospatial functions with the Rey figure copy test; (4) frontal-executive functions with the clock drawing test; and (5) learning and memory with Rey's word list immediate and delayed recall, Rey's figure delayed recall [10] and the three-objects-three-places tests [11]. The diagnosis of probable AD was made according to common research criteria [12].

Twenty cognitively healthy subjects were selected from those enrolled in a previous study [13], and these subjects underwent multidimensional assessment, including clinical, neurological and neuropsychological evaluations.

Written informed consent was obtained from patients and controls prior to their inclusion in the study. No compensation was provided for study participation. The study was approved by the local ethics committee and performed in accordance with the ethical standards laid down in the 1964 Declaration of Helsinki.

MR acquisition and post-processing

Magnetic resonance scans were acquired with a Philips Gyroscan 1.0 T scanner at the Neuroradiology Unit of the Città di Brescia Hospital. High-resolution gradient echo sagittal 3D sequences (TR = 20 ms, TE = 5 ms, flip angle 30°, field of view = 220 mm, acquisition matrix = 256 × 256 and slice thickness = 1.3 mm) were acquired. Gray matter was studied with the CPM algorithm developed at the Laboratory of Neuroimaging (LONI) of the University of California at Los Angeles [14].

Cortical mapping

The 3D images were reoriented along the AC–PC line and voxels below the cerebellum were removed with the MRIcro

software (http://www.sph.sc.edu/comd/rorden/mricro.html) in order to improve extraction of the cerebral cortex in areas adjacent to the cerebellum. The anterior commissure was manually set as the origin of the spatial coordinates for an anatomical normalization algorithm implemented in the Statistical Parametric Mapping (SPM99) software package (http://www.fil.ion.ucl.ac.uk/spm/). A 12-parameter affine transformation was used to normalize each image to a customized template in stereotaxic space, created from the MRI scans of 40 control subjects.

Individual brain masks for each hemisphere were extracted from normalized images with the automatic software Brainsuite (http://brainsuite.usc.edu), and visually inspected and manually corrected with *Display*, a three dimensional visualization program (http://www.bic.mni.mcgill.ca/software/Display/Display.html) that allows the manual correction of errors in differentiating brain and nonbrain tissues in regions of interest (or "masks"). The resulting masks were then applied to normalized images to obtain "skull-stripped" images of each hemisphere. After automated 3D hemispheric reconstruction using an intensity threshold that best differentiated gray matter from extracerebral CSF [15], a total of 39 sulcal lines for each hemisphere were manually traced (17 sulci on the lateral surface, 12 sulci on the medial surface and 10 lines drawn to outline interhemispheric gyral limits of each hemisphere) by a single tracer (A.P.) on the cortical surfaces, following a detailed and extensively validated protocol (http://www.loni.ucla.edu/~khayashi/Public/medial_surface/ ; http://www.loni.ucla.edu/~esowell/new_sulcvar.html) for each subject. The reliability of the manual outlining was assessed prior to experimental subject tracing with a standard protocol requiring the same rater to trace all lateral and medial sulci of six test brains [16]. At the end of the reliability phase, the mean 3D difference between the tracer and the gold standard [16] was <3 mm everywhere for medial and lateral sulci.

Individual sulcal maps were averaged to create a common average sulcal map for all subjects in the study [17]. The individual cortical surfaces were parameterized, flattened, and warped. Image voxels were classified using a partial volume classifier algorithm [18]. Gray matter volumes were extracted and mapped onto the corresponding parametric hemispheric model in exact spatial correspondence. Gray matter density was computed at each cortical point as the proportion of tissue classified as gray matter in a sphere of radius 15 mm centered at that point, and then averaged within each group to obtain the mean gray matter density.

Maps of the average percentage gray matter reduction were computed based on the ratio, at each cortical point, between the mean gray matter density value at that point in each patient group (iAD, miAD and moAD) and the mean gray matter density in the pertinent control group (iAD vs. OH, miAD vs. iAD, moAD vs. miAD). This ratio allows maps of the relative deficit in gray matter to be visualized, as a proportion or percentage of the normal values seen in healthy controls.

The reproducibility of the CPM technique is satisfactory. Sowell and colleagues [19] estimated the error in the cortical thickness measure that may be ascribed to repeated scanning, and found that it was around 0.15 mm.

Gray matter volumetry in the Brodmann areas

A deformable Brodmann area atlas [20] was applied to the left and right hemisphere average models (Fig. 1) (http://brainvis.wustl.edu/wiki/index.php/Caret:Download) [21].

Statistical analysis

Cortical pattern matching analyses were carried out to assess the relationship between gray matter density and diagnosis and thus identify cortical gray matter loss in (1) iAD compared to OH, (2) miAD compared to iAD, and (3) moAD compared to miAD. Maps of the percentage reduction and its significance were created. A surface point significance threshold of $P < 0.05$ was used to visualize the regional specificity of gray matter changes in the cortex. Correction for multiple comparisons was carried out by permutation testing at a threshold of $P = 0.01$. This analysis assesses the fraction of the cortical surface area with statistics exceeding the given threshold and compares it with a null distribution constructed empirically by randomly assigning subjects to groups [4]. The effect of gender distribution was controlled by performing two CPM analyses (older healthy vs. iAD, miAD and moAD pooled together) in men and women separately; the principal analyses were then repeated with gender and age added separately as covariates.

The possible confounding effect of age was controlled by excluding three miAD and three moAD patients whose ages at onset were below 65 years of age from our samples and then re-running the principal CPM analyses on the remaining patients.

Results

Table 1 shows that the patients and controls were generally in their 70s (no significant differences between groups for age); their mean educational level was between primary and middle school; and their global cognitive performance and the prevalence of ApoE-ε4 carriers were as expected based on the diagnostic categories. Gender was unbalanced, with

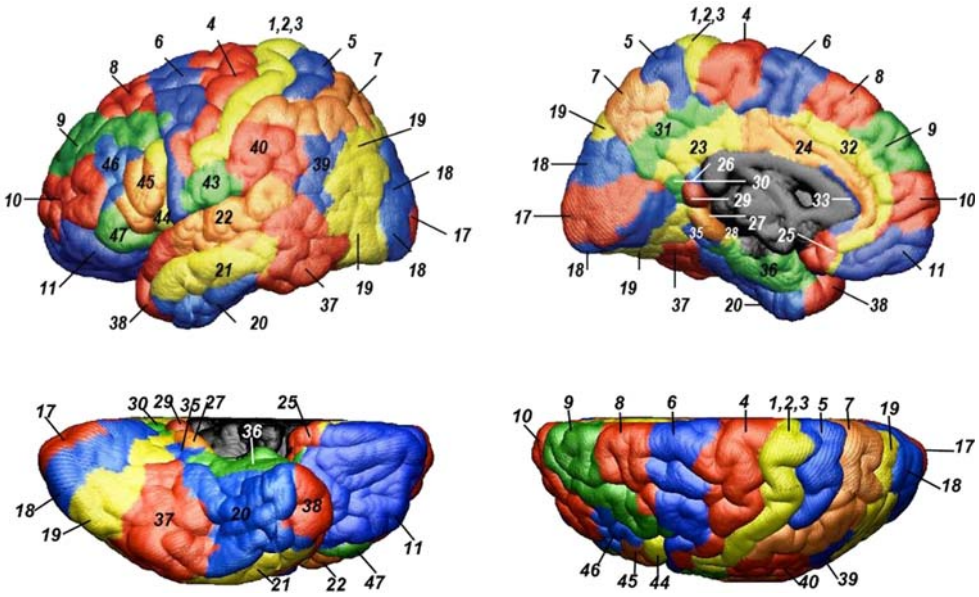

Fig. 1 3D rendering of the deformable atlas used to compute gray matter volumes in the Brodmann areas [19]

Table 1 Sociodemographic, cognitive, genetic and neuropsychological features of the study groups

	Older healthy ($N = 20$)	Incipient AD ($N = 11$)	Mild AD ($N = 15$)	Moderate AD ($N = 15$)
Sociodemographic, cognitive, and genetic features of the study groups				
Age (years)	73.9 ± 7.9	77.6 ± 5.6	72.7 ± 8.9	73.4 ± 9.5
Gender, female (%)	14 (70%)	3 (27%)	9 (60%)	13 (87%)
Education (years)	9.0 ± 4.5	8.5 ± 4.5	7.1 ± 5.6	5.2 ± 2.1
Mini-mental state exam [range]	29.1 ± 1.0 [30–27]	26.5 ± 2.0 [29–24]	23.5 ± 2.2 [27–20]	16.5 ± 2.0 [19–13]
ApoE-ε4 carriers, *N* (%)	4/20 (20%)	5/11 (45%)	5/15 (33%)	7/13 (54%)
Neuropsychological tests				
Learning				
Rey's list immed. recall	41.8 ± 6.9*	26.2 ± 6.5†	19.7 ± 7.1$^{\#}$	14.0 ± 6.2$^{\#}$
Delayed recall	8.2 ± 3.6*	2.6 ± 1.6†	1.7 ± 2.0†	0.9 ± 0.1†
Rey's figure recall	15.2 ± 7.4*	5.7 ± 4.5†	2.1 ± 2.6†	0.8 ± 1.5$^{\bullet}$
Three objects three places	8.7 ± 0.8*	7.1 ± 2.3†	3.8 ± 2.8$^{\#}$	2.1 ± 2.4$^{\bullet}$
Language				
Token	31.8 ± 3.0*	31. 7 ± 2.8*	30. 7 ± 5.0*	21.5 ± 5.3$^{\bullet}$
Category fluency	35.9 ± 11.0*	24.9 ± 5.4†	18.8 ± 9.8$^{\#}$	13.9 ± 4.4$^{\#}$
Frontal-exec.				
Clock drawing	1.9 ± 1.1*	2.3 ± 1.1*	3.8 ± 1.5$^{\#}$	5.3 ± 0.7$^{\#}$
Visuospatial				
Rey's figure copy	31.9 ± 6.4*	31.1 ± 2.9*	13.9 ± 11.3$^{\#}$	6.2 ± 8.5$^{\bullet}$

Values indicate mean ± SD. Neuropsychological tests scores are adjusted for age, sex and education

*, †, $^{\#}$,$^{\bullet}$ No or the same markers denote no differences, while different markers denote significant differences on one-way ANOVA with Tukey's post hoc comparisons

the prevalence of females being highest in the moAD group and lowest in iAD. Cholinesterase inhibitors were taken by none of the iAD, 6/15 (40%) of the miAD and 8/15 (53%) of the moAD subjects.

Neuropsychological performance revealed increasing cognitive impairment from OH through to iAD, miAD, and moAD (Table 1). However, memory and language production tests were sensitive to changes as early as the iAD stage, while language comprehension, frontal-executive, and visuospatial tests declined at more advanced stages.

Figure 2 shows that, compared to OH, iAD subjects featured a cortical gray matter loss of up to 20–30% in the

medial temporal, posterior cingulate/retrosplenial, and subgenual/orbitofrontal cortices, and a less widespread loss of up to 15–20% in the temporoparietal regions ($P = 0.0004$ on permutation testing). Tissue loss in the medial temporal cortex reached values of >30% in a very restricted area corresponding to the right entorhinal cortex; however, this failed to achieve statistical significance on a voxel-by-voxel basis (see Fig. 2). Compared to iAD, miAD featured widespread lateral temporal, temporoparietal, dorsal parietal, dorsal frontal, and occipital gray matter losses of 30% and above, with less marked losses in the medial temporal (lower than 10–20%) and posterior cingulate/retrosplenial regions (lower than 10–15%, $P < 0.0001$). Compared to miAD, moAD featured a gray matter loss of up to 25–30% in the primary sensorimotor cortex ($P = 0.04$), with the losses in the temporal, parietal, and frontal regions being markedly lower (below 10%).

Table 2 shows the average volume percent differences between groups in ROI defined in terms of Brodmann areas. As expected, the atrophy pattern is similar to that outlined in Fig. 2, although the values, being area averages, are always lower. Compared to OH, the iAD group featured cortical gray matter reductions of 12–20% in the posterior cingulate/retrosplenial and subgenual/orbitofrontal cortices, a less widespread loss of 9–13% in the medial temporal, and 5–11% losses in other cortical areas. The largest losses were in BA23 and BA31 (data not shown), where the gray matter losses were 21–18% to the left–right and 17–19%, respectively. The gray matter loss of miAD versus iAD in the fronto-temporal–parietal cortex was between 14 and 19%, in the medial temporal cortex it was 9–13%, and in the posterior cingulate/retrosplenial regions it was 7–9%. Atrophy in the primary sensorimotor cortex of moAD versus miAD was 10–11%, while the losses in almost all other regions were below 10%.

The effect of gender was controlled for by computing gray matter volumes in the regions of interest listed in Table 2 separately for men and women in older healthy persons and AD patients. None of the comparisons was significant by the Mann–Whitney U test, indicating that gender was not a confounder for the findings of this study.

Moreover, the effects of gender and age were controlled for by performing two CPM analyses with age and then gender as covariates. The results, although less marked,

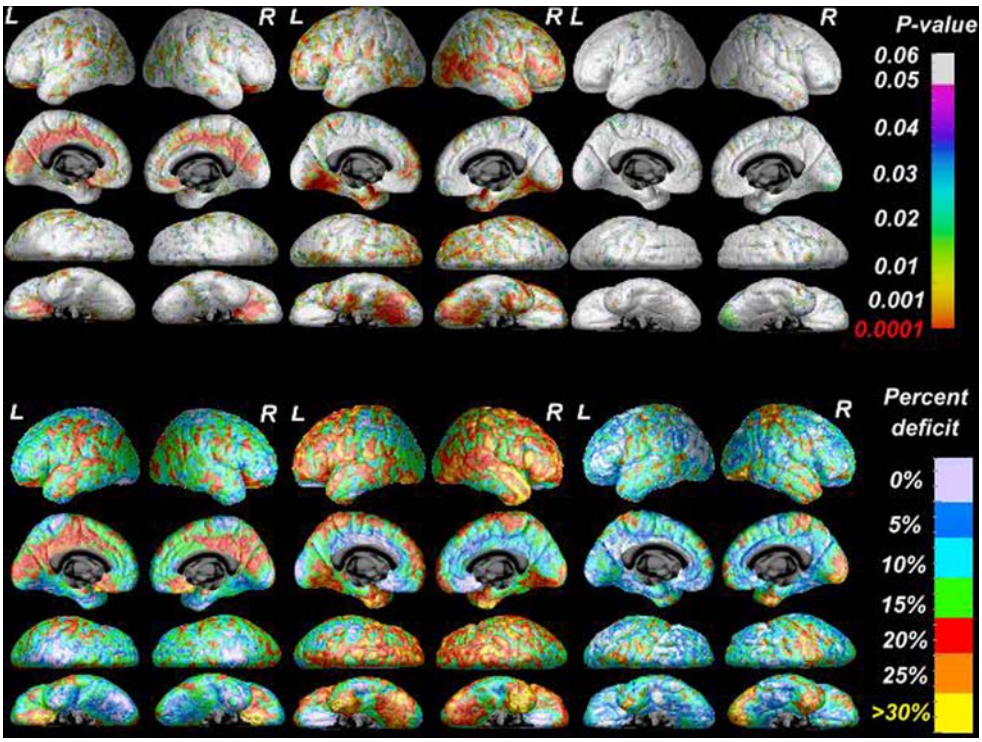

Fig. 2 Incremental gray matter loss from incipient through to mild and moderate AD. *Upper rows* denote significance maps and *lower rows* percentage differences. Incipient AD features a cortical gray matter loss of 20–30% in the medial temporal, posterior cingulate/retrosplenial, subgenual/orbitofrontal cortices, and a less widespread loss of 15–20% in the temporoparietal region. Compared to incipient, mild AD featured widespread temporal, temporoparietal, dorsal parietal, and dorsal frontal gray matter losses of 30% and above, with less marked losses in the medial temporal (10–20%) and posterior cingulate/retrosplenial regions (10–15%). Compared to mild AD, moderate AD featured gray matter losses of 25–30% in the primary sensorimotor and visual cortices, with the losses in the temporal, parietal, and frontal regions being markedly lower (below 10%)

Table 2 Incremental regional gray matter loss from incipient through to mild and moderate AD in selected areas

Regions of interest	Brodmann areas		Incipient AD versus older healthy (%)	Mild AD versus incipient AD (%)	Moderate AD versus mild AD (%)
Posterior cingulate/ retrosplenial cortex	BA23 31 posterior cingulate	L	−14***	−7	−3
	BA26 29 30 retrosplenial	R	−12**	−9	−2
Subgenual/orbitofrontal cortex	BA11 prefrontal orbital cortex, BA25 subgenual cortex	L	−13***	−9	−3
		R	−20***	−5	−7
Medial temporal cortex	BA27 presubiculum, BA28 entorhinal cortex, BA35 perirhinal cortex, BA36 perirhinal cortex	L	−9*	−13***	−0.5
		R	−13***	−9	−6
Temporal pole	BA20 inferior temporal gyrus, BA38 temporal pole	L	−5	−18**	−7
		R	−7	−19***	−12
Dorsal frontal cortex	BA6 8 9 superior frontal gyrus, BA10 frontopolar cortex, BA44 45 inferior frontal gyrus, BA46 middle frontal gyrus, BA47 orbital cortex (lateral)	L	−7	−19***	−5
		R	−9	−16***	−6
Dorsal temporal cortex	BA21 middle temporal gyrus, BA22 superior temporal gyrus (posterior), BA37 fusiform gyrus	L	−8	−16***	−6
		R	−10	−17***	−6
Temporal parietal cortex	BA5 secondary somatosensory cortex, BA7 precuneus, BA39 angular gyrus, BA40 inferior parietal lobule	L	−8	−14***	−6
		R	−11	−15***	−8
Sensorimotor cortex	BA1 2 3 4 43 primary motor and somatosensory cortex	L	−7	−17***	−10**
		R	−11	−14***	−11**
Visual cortex	BA17 primary visual cortex, BA18 19 associative visual cortex	L	−8	−15***	−5
		R	−11	−14***	−8

Percentages denote volume differences computed in Brodmann regions of interest defined via a deformable brain atlas [19]

BA, Brodmann area; *L*, left; *R*, right

Significant differences at * $P < 0.05$, ** $P < 0.01$, and *** $P < 0.001$ on nonparametric Mann–Whitney *U* test

were basically unchanged, suggesting that atrophy is slightly affected by age and gender (see Figure 3 at Supplementary material).

The third CPM analysis, in which three miAD and three moAD patients whose ages at onset were less than 65 years old were excluded from the sample, revealed the same pattern of cortical gray matter deficit observed in the principal analyses, although the results were less powerful ($P = 0.0001$ on permutation testing for both left and right hemispheres in iAD vs. miAD comparison; $P = 0.06$ for the left and $P = 0.05$ for the right hemispheres in miAD vs. moAD comparison; see Figure 4 at Supplementary material).

Discussion

The most marked reductions in cortical volume observed in the maps occurred in the posterior cingulate/retrosplenial and subgenual/orbitofrontal cortex in iAD, the dorsal frontal–temporal–parietal–occipital cortex in miAD, and the sensorimotor cortex in moAD. At each severity stage, the reduction in cortical volume is lower elsewhere, consistent with the view that waves of atrophy affect different brain networks at different times over the course of AD (Table 3).

The topography of the atrophy found in iAD and miAD suggests involvement of the polysynaptic and direct intrahippocampal pathways, respectively. The synaptic stations of the first pathway are the entorhinal cortex, the gyrus dentatus, the cornu Ammonis, and the subiculum, where efferent fibers project to the posterior cingulate/retrosplenial cortex [22]. The synaptic stations of the direct intrahippocampal pathway are the entorhinal cortex, the CA1 subfield, and the subiculum, where efferent fibers project to the temporal pole and the inferior temporal associative and prefrontal cortex [22]. This view agrees well with the notion that the first pathway is involved in encoding episodic and spatial memories, the second pathway is involved in encoding semantic memories [22], and that episodic and spatial memories are affected at earlier and semantic memories at later stages of AD. We hypothesize that serial involvement of the polysynaptic and direct pathways over the course of the disease is the

Table 3 Hypothetical neural networks affected by AD at the different stages of disease severity as suggested by the results of the present study

Disease stage	Neural system	Involved cortical areas	Function
Incipient AD	Polysynaptic hippocampal pathway	Posterior cingulate and retrosplenial cx	Encoding episodic and spatial memories
		Entorhinal cx	
	Olfactory	Subgenual/orbitofrontal cx	Smell discrimination
Mild AD	Direct hippocampal pathway	Temporal pole	Encoding semantic memories
		Inferior temporal associative cx	
		Prefrontal cx	
		Entorhinal cx	
	Sensorimotor network	Primary sensorimotor cx	Control of motor schemes and discriminatory sensory perception
	Visual network	Primary and associative visual cx	Visual discrimination
Moderate AD	Sensorimotor network	Primary sensorimotor cx	Control of motor schemes and discriminatory sensory perception

pathophysiological phenomenon underlying our structural findings. The hypothesis that discrete networks are selectively affected at different disease stages is supported by the inversion of the ratio between the posterior cingulate/retrosplenial and dorsal/lateral frontal–temporal–parietal regions in iAD and miAD. While the posterior cingulate/retrosplenial region is heavily atrophic in iAD relative to OH, incremental atrophy in miAD is much lower, the opposite pattern occurring in the dorsal/lateral frontal–temporal–parietal regions.

Areas other than those involved in the polysynaptic and direct intrahippocampal pathways are also involved in iAD and miAD. Atrophy of the subgenual/orbitofrontal cortex, involved in the perception of smell [23], have repeatedly been found in patients with MCI and overt AD [24], while smell discrimination seems to be reduced early during the course of the disease [25], and pathologic data indicate that this area is heavily affected by tangle [26] and amyloid pathology [27]. Interestingly, atrophy in the orbitofrontal cortex of AD patients has been found to be more severe in men than in women [28]. This observation is consistent with the greater prevalence of men in iAD than OH in our study.

It should be underlined that atrophy in miAD also encompasses the primary sensorimotor and visual cortex. Traditionally, primary cortices are affected by pathology in the more advanced stages of AD [29]. However, pathological studies on the distribution of senile plaques in AD [30] found that the primary visual areas are more affected by neuronal death and glial proliferation than previously reported, while the striate cortex exhibits a higher density of senile plaques [31]. Moreover, a study on visual behavior in AD found a selective loss of higher-order visual functions that was not attributable to retinal or optic nerve lesions [32].

The primary sensorimotor cortex is the only area undergoing significant incremental atrophy at the stage of moAD. Some studies have found subclinical signs of dysfunction of this cortex at relatively early stages of the disease. Perretti and colleagues [33] used motor evoked potentials (MEPs) on the motor cortices of 15 mild and moderate AD patients and found abnormally high MEP thresholds in 40% of the patients. The reason why motor symptoms only appear late in the disease process may be the greater capacity of this region to undergo plastic changes that preserve function [34]. Our finding is all the more significant in view of the normally thinner cortex in this area [4, 35]. Notably, in moAD, incremental atrophy in the medial temporal lobe was minimal, averaging -0.5 to -2%, and indicating that the greatest share of damage to this area occurs at the iAD and miAD stages.

The slowdown in atrophy that we detected may be an artifact due to the decreased sensitivity of the MR approach in a brain with continuously accelerating atrophy. However, neuropathological data indicate that brain atrophy at death is lower than in a predictive model that assumes a continuous acceleration of atrophy [36]. Alternatively, volume loss may decelerate due to the incremental deposition of space-occupying amyloid [37, 38], and atrophy then results from the balance between increased amyloid and neuronal and axonal loss. While this is a plausible scenario, explaining why this balance changes over the disease course at different rates in different brain regions and how tangle deposition contributes to tissue loss remains guesswork. Lastly, the naturally asymptotic

decrease in atrophy rates invoked to explain the deceleration of atrophy in small structures does not seem pertinent to the cortical gray matter [39].

The major limitation of this study is that our data are cross-sectional, and all inferences should be confirmed by others with a prospective design and possibly with groups that are more homogeneous by gender and education [40]. Moreover, the possible contribution of age at disease onset to the observed patterns of regional cortical atrophy should be taken into account, given the greater atrophy known to occur when AD starts before age 65 [41] and the slightly older age of our iAD group. Although we statistically controlled for the effects of age and gender, more studies in groups of patients better balanced by age and gender are needed. The image acquisition protocol and post-processing methods used are not immediately comparable with other similar reports [2], although their reproducibility and stability over time seem to be quite good [19]. Other studies have mapped atrophy at different disease stages but have neither assessed incremental atrophy through stages of increasing disease severity nor estimated the proportion of tissue loss [6]. However, this limitation is shared by all studies predating the harmonization effort of the Alzheimer's Disease Neuroimaging Initiative (ADNI) [42], which developed acquisition protocols of comparable accuracy for a number of MR scanners. Coupling the ADNI standard protocol with a standard method to measure brain volume changes will provide scientists with a powerful tool to track AD progression. Obviously, future studies with serial scans will need to overcome the intrinsic limitation of this cross-sectional one. However, the longitudinal data of the public ADNI dataset available at the time of this writing (December 2008) allows only narrow severity windows (24 months at most in a handful of subjects; 30 months in no one yet) to be investigated, which is in no way as wide as the normal-to-moderate AD severity window that we investigated cross-sectionally in this study, and it will not be this wide for a few years to come.

Mapping incremental atrophy in AD has shown that cortical atrophy follows a region-specific pattern of acceleration–deceleration. Datasets that are being compiled with serial scans starting from iAD and extending over many years will allow the pattern of acceleration–deceleration of atrophy to be mapped in finer detail, which may serve as a statistical reference for therapeutic interventions aimed at modifying disease progression.

Acknowledgments We wish to thank Francesca Sabattoli for help in the inter-rater reliability of cortical pattern matching, and Michela Pievani for continuous technical and logistic support.

Conflict of interest statement The authors report no conflicts of interest.

References

1. Committee for Medicinal Products for Human Use (CHMP) (2007) Guideline on medicinal products for the treatment of Alzheimer's disease and other dementias (draft; CPMP/EWP/553/95 Rev. 1). CHMP, London
2. Ridha BH, Barnes J, Bartlett JW, Godbolt A, Pepple T, Rossor MN, Fox NC (2006) Tracking atrophy progression in familial Alzheimer's disease: a serial MRI study. Lancet Neurol 5:828–834
3. Whitwell JL, Shiung MM, Przybelski SA, Weigand SD, Knopman DS, Boeve BF, Petersen RC, Jack CR Jr (2008) MRI patterns of atrophy associated with progression to AD in amnestic mild cognitive impairment. Neurology 70:512–520
4. Thompson PM, Hayashi KM, de Zubicaray G, Janke AL, Rose SE, Semple J, Herman D, Hong MS, Dittmer SS, Doddrell DM, Toga AW (2003) Dynamics of gray matter loss in Alzheimer's disease. J Neurosci 23:994–1005
5. Smith AD (2002) Imaging the progression of Alzheimer pathology through the brain. Proc Natl Acad Sci USA 99:4135–4137
6. Whitwell JL, Przybelski SA, Weigand SD, Knopman DS, Boeve BF, Petersen RC, Jack CR Jr (2007) 3D maps from multiple MRI illustrate changing atrophy patterns as subjects progress from mild cognitive impairment to Alzheimer's disease. Brain 130:1777–1786
7. Du AT, Schuff N, Amend D, Laakso MP, Hsu YY, Jagust WJ, Yaffe K, Kramer JH, Reed B, Norman D, Chui HC, Weiner MW (2001) Magnetic resonance imaging of the entorhinal cortex and hippocampus in mild cognitive impairment and Alzheimer's disease. J Neurol Neurosurg Psychiatry 71:441–447
8. Chételat G, Desgranges B, De La Sayette V, Viader F, Eustache F, Baron JC (2002) Mapping gray matter loss with voxel-based morphometry in mild cognitive impairment. Neuroreport 13:1939–1943
9. Petersen RC, Doody R, Kurz A, Mohs RC, Morris JC, Rabins PV, Ritchie K, Rossor M, Thal L, Winbald B (2001) Current concepts in mild cognitive impairment. Arch Neurol 58:1985–1992
10. Lezak M, Howieson D, Loring DW (2004) Neuropsychological assessment, 4th edn. University Press, Oxford
11. Prestia A, Rossi R, Geroldi C, Galluzzi S, Ettori M, Alaimo G, Frisoni GB (2006) Validation study of the three-objects-three-places test: a screening test for Alzheimer's disease. Exp Aging Res 32:395–410
12. McKhann G, Drachman D, Folstein M, Katzman R, Price D, Stadlan EM (1984) Clinical diagnosis of Alzheimer's disease: report of the NINCDS-ADRDA Work Group under the auspices of Department of Health and Human Services Task Force on Alzheimer's Disease. Neurology 34:939–944
13. Riello R, Sabattoli F, Beltramello A, Bonetti M, Bono G, Falini A, Magnani G, Minonzio G, Piovan E, Alaimo G, Ettori M, Galluzzi S, Locatelli E, Noiszewska M, Testa C, Frisoni GB (2005) Brain volumes in healthy adults aged 40 years and over: a voxel-based morphometry study. Aging Clin Exp Res 17:329–336
14. Thompson PM, Hayashi KM, De Zubicaray GI, Janke AL, Rose SE, Semple J, Hong MS, Herman DH, Gravano D, Doddrell DM, Toga AW (2004) Mapping hippocampal and ventricular change in Alzheimer disease. Neuroimage 22(4):1754–1766; erratum (2007) 36:1397–1398
15. Heilbrun MP, Koehler S, MacDonald P, Siemionow V, Peters W (1994) Preliminary experience using an optimized three-point transformation algorithm for spatial registration of coordinate systems: a method of noninvasive localization using frame-based stereotactic guidance systems. J Neurosurg 81:676–682

16. Sowell ER, Thompson PM, Rex D, Kornsand D, Tessner KD, Jernigan TL, Toga AW (2001) Mapping continued brain growth and gray matter density reduction in dorsal frontal cortex: Inverse relationships during postadolescent brain maturation. J Neurosci 21:8819–8829
17. Thompson PM, Woods RP, Mega MS, Toga AW (2000) Mathematical/computational challenges in creating deformable and probabilistic atlases of the human brain. Hum Brain Mapp 9:81–92
18. Shattuck DW, Leahy RM (2001) Automated graph-based analysis and correction of cortical volume topology. IEEE Trans Med Imaging 20:1167–1177
19. Sowell ER, Thompson PM, Leonard CM, Welcome SE, Kan E, Toga AW (2004) Longitudinal mapping of cortical thickness and brain growth in normal children. J Neurosci 24:8223–8231
20. Rasser PE, Johnston P, Lagopoulos J, Ward P, Schall U, Thienel R, Bender S, Toga A, Thompson PM, Functional MRI (2005) BOLD response to Tower of London performance of first-episode schizophrenia patients using cortical pattern matching. Neuroimage 26:941–951
21. Van Essen DC (2002) Windows on the brain. The emerging role of atlases and databases in neuroscience. Curr Opin Neurobiol 12:574–579
22. Duvernoy HM (1998) The human hippocampus: functional anatomy, vascularization and serial sections with MRI. Springer, New York, pp 29–30
23. Yousem DM, Williams SC, Howard RO, Andrew C, Simmons A, Allin M, Geckle RJ, Suskind D, Bullmore ET, Brammer MJ, Doty RL (1997) Functional MR imaging during odor stimulation: preliminary data. Radiology 204:833–838
24. Chételat G, Landeau B, Eustache F, Mézenge F, Viader F, de la Sayette V, Desgranges B, Baron JC (2005) Using voxel-based morphometry to map the structural changes associated with rapid conversion in MCI: a longitudinal MRI study. Neuroimage 27:934–946
25. Djordjevic J, Jones-Gotman M, De Sousa K, Chertkow H (2008) Olfaction in patients with mild cognitive impairment and Alzheimer's disease. Neurobiol Aging 29:693–706
26. Salat DH, Kaye JA, Janowsky JS (2001) Selective preservation and degeneration within the prefrontal cortex in aging and Alzheimer disease. Arch Neurol 58:1403–1408
27. Resnick SM, Lamar M, Driscoll I (2007) Vulnerability of the orbitofrontal cortex to age-associated structural and functional brain changes. Ann N Y Acad Sci 1121:562–575
28. Callen DJ, Black SE, Caldwell CB, Grady CL (2004) The influence of sex on limbic volume and perfusion in AD. Neurobiol Aging 25:761–770
29. Braak H, Braak E, Bohl J (1993) Staging of Alzheimer-related cortical destruction. Eur Neurol 33:403–408
30. Kuljis RO, Tikoo RK (1997) Discontinuous distribution of senile plaques within striate cortex hypercolumns in Alzheimer's disease. Vision Res 37:3573–3591
31. Suvà D, Favre I, Kraftsik R, Esteban M, Lobrinus A, Miklossy J (1999) Primary motor cortex involvement in Alzheimer disease. J Neuropathol Exp Neurol 58:1125–1134
32. Cronin-Golomb A, Rizzo JF, Corkin S, Growdon JH (1991) Visual function in Alzheimer's disease and normal aging. Ann N Y Acad Sci 640:28–35
33. Perretti A, Grossi D, Fragassi N, Lanzillo B, Nolano M, Pisacreta AI, Caruso G, Santoro L (1996) Evaluation of the motor cortex by magnetic stimulation in patients with Alzheimer disease. J Neurol Sci 135:31–37
34. Ferreri F, Pauri F, Pasqualetti P, Fini R, Dal Forno G, Rossini PM (2003) Motor cortex excitability in Alzheimer's disease: a transcranial magnetic stimulation study. Ann Neurol 53:102–108
35. Lerch JP, Pruessner JC, Zijdenbos A, Hampel H, Teipel SJ, Evans AC (2005) Focal decline of cortical thickness in Alzheimer's disease identified by computational neuroanatomy. Cereb Cortex 15:995–1001
36. Double KL, Halliday GM, Kril JJ, Harasty JA, Cullen K, Brooks WS, Creasey H, Broe GA (1996) Topography of brain atrophy during normal aging and Alzheimer's disease. Neurobiol Aging 17:513–521
37. Fox NC, Black RS, Gilman S, Rossor MN, Griffith SG, Jenkins L, Koller M, AN1792(QS-21)-201 Study (2005) Effects of Abeta immunization (AN1792) on MRI measures of cerebral volume in Alzheimer disease. Neurology 64:1563–1572
38. Hock C, Nitsch RM (2005) Clinical observations with AN-1792 using TAPIR analyses. Neurodegener Dis 2:273–276
39. Scahill RI, Schott JM, Stevens JM, Rossor MN, Fox NC (2002) Mapping the evolution of regional atrophy in Alzheimer's disease: unbiased analysis of fluid-registered serial MRI. Proc Natl Acad Sci USA 99:4703–4707
40. Pakkenberg B, Gundersen HJ (1997) Neocortical neuron number in humans: effect of sex and age. J Comp Neurol 384:312–320
41. Frisoni GB, Pievani M, Testa C, Sabattoli F, Bresciani L, Bonetti M et al (2007) The topography of grey matter involvement in early and late onset Alzheimer's disease. Brain 130:720–730
42. Mueller SG, Weiner MW, Thal LJ, Petersen RC, Jack CR, Jagust W, Trojanowski JQ, Toga AW, Beckett L (2005) Ways toward an early diagnosis in Alzheimer's disease: the Alzheimer's Disease Neuroimaging Initiative (ADNI). Alzheimers Dement 1:55–66